

Measurements of the steady streaming flow around oscillating spheres using 3D particle tracking velocimetry

Florian Otto,* Emmalee K. Riegler, and Greg A. Voth
Department of Physics, Wesleyan University, Middletown CT 06459, U.S.A.[†]
 (Dated: July 29, 2021)

Granular particles vibrated in a fluid have been found to exhibit self-organization with attractive and repulsive interactions between the particles. These interactions have been attributed to the steady streaming flow around oscillating particles. Here we examine the steady streaming flow surrounding a vertically oscillating sphere using three dimensional particle tracking velocimetry. We present measurements of the flow with the sphere far from boundaries, close to the bottom wall of the tank, and near another oscillating sphere. The steady velocity field is found to disagree with available analytic calculations. When the sphere is oscillated near the bottom wall the entire topology of the flow changes, resulting in a larger repulsive region than expected. Previous experiments saw attraction between particles in the region where the flow around a single particle is repulsive. We conclude that advection in the streaming flow due to a single particle cannot explain the observed attractive and repulsive interactions, rather non-linear interactions between the flows around two or more spheres must be responsible.

I. INTRODUCTION

Steady streaming flows due to the oscillatory motion of a fluid are responsible for a wide range of fluid phenomena. Work on this problem goes back to Rayleigh¹. Applications of steady streaming flows include driving fluid with ultrasonic beams², microfluidic transport³, vesicle license⁴, and streaming flows in the ear⁵.

Recent experiments have observed self-organization of granular particles when they are vibrated vertically^{6,7} or horizontally⁸ in a fluid. Streaming flows were identified as the mechanism for self-organization, but there remained puzzling questions about the structure of the streaming flows and the attractive and repulsive interactions between particles. In this paper we present experimental 3D particle tracking measurements of the flow around vertically oscillating spheres. We show that for a streaming flow far from boundaries the available analytic solutions do not agree with our measurements, likely because the theories are for limiting cases that are far from the experimental parameters. Measurements of the streaming flow at different distances from a solid bottom wall reveal that the wall changes the topology of the streaming flow. We also present measurements of the flow around two oscillating spheres.

II. PARAMETER SPACE FOR OSCILLATING SPHERES

In Figure 1 we show the parameter space relevant for a single oscillating sphere far from any boundaries. The vertical axis is the oscillation amplitude (half peak to peak) nondimensionalized by the particle radius,

$$\epsilon = A/a . \quad (1)$$

The horizontal axis is the Reynolds number,

$$Re = A\omega 2a/\nu . \quad (2)$$

Analytical solutions of the steady streaming flow around an oscillating sphere have three limits, which are indicated by Roman numerals in Figure 1. The theoretical calculations are usually described in terms of alternate nondimensional parameters

$$M^2 = \frac{Re}{\epsilon} = \frac{2a^2}{\nu/\omega} \quad (3)$$

$$Re_s = \epsilon Re = \frac{2A^2}{\nu/\omega} .$$

The quantity $\delta_{osc} = \sqrt{\nu/\omega}$ is the thickness of the oscillatory boundary layer. In Fig. 1, solid lines are drawn at $M^2 = 1$ (upward sloping) and $Re_s = 1$ (downward sloping). The analytical solutions in limits I and II were found by Riley¹⁰. Both these solutions are in the limit

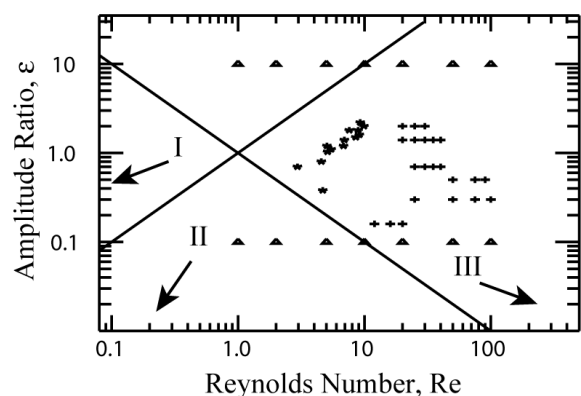


FIG. 1: Parameter space for a single oscillating sphere in an infinite fluid. Plus symbols indicate data from this study; asterisk indicate data from Voth et. al⁶; triangles indicate data from Blackburn⁹. The Roman numerals indicate the limits described in Section II for which calculations of the steady stream flow field are available.

of small Re_s (so that the streaming flow is dominated by viscosity) and small ϵ (so that the oscillation amplitude is infinitesimal). The solution in limit I requires $M^2 \ll 1$ so that the oscillatory boundary layer thickness is much larger than the size of the sphere. In this limit the streaming flow is inward along the oscillation axis and outward at the equator. The solution in limit II requires $M^2 \gg 1$ so that the oscillatory boundary layer is much smaller than the sphere size. Here the streaming flow has an inner recirculation zone and an oppositely directed outer recirculation zone that flows inward toward the equator and outward along the oscillation axis (see Van Dyke¹¹ or Fig. 3 for images of this flow). Solution III was obtained by Brenner and Stone⁶, who assume that the outer streaming flow is potential flow ($Re_s \gg 1$ and $\epsilon \ll 1$). The flow field here is qualitatively similar to Solution II.

The symbols in Fig. 1 show the parameters of the experiments in this paper, Voth et. al⁶, and the simulations by Blackburn⁹. Despite agreement between Solution III and experiments on spheres bouncing above a vibrating plate⁶, we will see that the existing theories are inadequate to quantitatively describe the streaming flows in our experiments. Factors that contribute to the discrepancy include the non-infinitesimal oscillation amplitude, the intermediate Reynolds number of the streaming flow, the effects of the bottom wall, and non-linear interactions between the flow around two spheres.

III. EXPERIMENTAL SETUP

A diagram of the experiment is shown in Figure 2. The sphere is held in the center of an octagonal plexiglas tank. The tank has an inner diameter of 30 cm and a height of 20 cm. The octagonal shape was chosen because it nearly has cylindrical symmetry, but still provides eight flat walls for optical access. The sphere is attached to a thin rod that moves on a linear motion rail. The vertical oscillations are driven by a stepper motor as shown in Fig. 2(b). We primarily used a 1.91 cm diameter sphere attached to a 0.16 cm diameter rod. For some experiments we used a larger 5.09 cm sphere on a 0.33 cm rod. The vertical position of the sphere and the amplitude of the stroke could be adjusted continuously. The tank was filled with a mixture of glycerol and water, adjusted to give the required viscosity.

Three-dimensional particle tracking (3DPTV) was used to reconstruct the three dimensional positions and the velocities of the particles in the flow from stereoscopic camera images¹². 3DPTV has become a standard technique in many areas of fluid measurement, particularly in the study of turbulent flows^{13,14,15}. As we show here, it can also be used to rapidly map the full three dimensional flow field of simpler flows. Compared with PIV, 3DPTV requires lower seeding density, so it has lower spatial resolution. For periodic flows like ours, phase averaging can be used to obtain high spatial resolution for

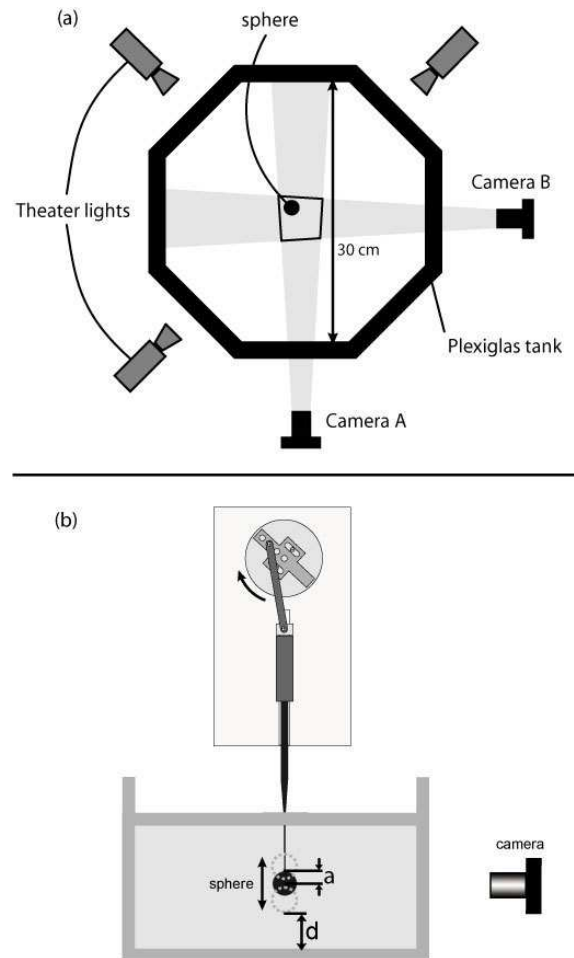


FIG. 2: (a) A top view of the experimental setup drawn to scale. Two cameras at 90° from each other provide a stereoscopic view of a volume of the the flow around the oscillating sphere. The overlap of the cameras is indicated by the quadrilateral. Three theater lights provide symmetric illumination for both cameras. (b) A side view of the setup not drawn to scale. The circular motion of the disk sitting on a stepper-motor is converted to a linear up-and-down motion by the use of a connecting rod and a linear motion rail. The distance between the lowermost point of the sphere during its stroke and the bottom plate will be referred to as d .

the full three dimensional flow field from a single data set. We have implemented a simple 3DPTV setup using two 1.3 Megapixel high-speed cameras for stereoscopic imaging. This limits the seeding density to significantly less than is possible with 3 or 4 cameras¹², but the setup was sufficient for our needs. Each camera has 4 GB of RAM which allowed 3200 images to be acquired continuously. The cameras imaged a volume surrounding the sphere roughly $8 \times 8 \times 8 \text{ cm}^3$ as shown in Fig. 2(a). The tracer particles were alumino-silicate microspheres 80-120 μm in diameter with density 0.7-0.9 g/cm^3 (supplied by Trelleborg Fillite, Inc.). Three 750 Watt theater lights gave symmetric illumination.

To find the three dimensional coordinates of the tracer particles, we match the image of a particle on one camera to the image of the same particle on the other camera. Each position on a camera image corresponds to a particle that exists somewhere along a ray in space. The three dimensional position of the particle is determined by finding rays from the two cameras that intersect. Converting image positions to rays in space requires a camera model and an accurate calibration to determine the parameters of the model. We used a simple distortion free camera model with seven parameters defining camera location, viewing direction, rotation and magnification. To obtain the calibration parameters, we imaged a calibration mask in the glycerol mixture and measured the real space positions of each dot. A non-linear fit of these measured positions to the calibration model gives the necessary calibration parameters for that camera. The system could determine the three dimensional position of a $100 \mu m$ particle with an accuracy of about $10 \mu m$.

Since we are primarily interested in the streaming flow created by the oscillatory motion of spheres, we typically take one image per period of the sphere oscillation. Tracking particles through these phase locked images allows direct measurement of the steady flow. The cameras were triggered by a photogate aligned with 16 uniformly spaced holes around the circular disk. Usually we covered all but one hole to resolve only the streaming flow. For some experiments we took 16 images per period to observe the oscillatory flow, i.e. how the recirculation zones changed during one driving cycle.

Experimental difficulties limited our access to the full parameter space of our problem. Firstly, the rod which is attached to and drives the sphere had some influence on the flow field. It produced an up/down asymmetry in the streaming flow even when the sphere was far from the wall, where up/down symmetry is usually expected. This effect became less important as Re_s was increased. Secondly, the continuous input of heat from the theater lights caused some convection in the fluid. We installed infrared mirrors and absorbing glass, but where the streaming flow is very weak (at small Re , small ϵ , or far from the sphere) the turbulent convective flow is still visible in the data. Finally, at high glycerol concentrations (for many runs we used 92% glycerol) we found that the index of refraction of the fluid became large enough that polystyrene particles, which we had planned to use as tracer particles, became invisible. The replacement particles had a density of $(0.7 - 0.9 g/cm^3)$ which was significantly less than that of the fluid $(1.24 g/cm^3)$, so the particles would rise very slowly due to buoyancy. This had a negligible effect on the measured velocities, but after a long experimental run, there would be no tracer particles left in the region around the sphere. All three of these problems were less significant for strong streaming flows at higher Re and ϵ . This is why our data is at higher Reynolds numbers than the data of Voth et. al⁶ and why we did not measure smaller ϵ to more directly compare with the analytical results (see Fig. 1).

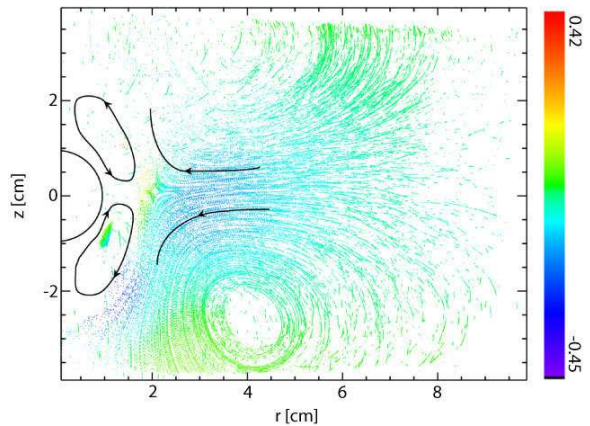


FIG. 3: Streaming flow pattern in the center of the tank at $Re = 30$ and $A/a = 1.4$. The plot shows height vs. radial position and the color indicates the radial velocity component, v_r . The position and size of the sphere are indicated by the semicircle.

IV. EXPERIMENTAL RESULTS

We first looked at the flow field around a single sphere oscillating in the center of the tank, where no boundaries should affect the flow. We went on to study the changes that result from the presence of the bottom plate, where we observed a dramatic change in the flow topology. The last set of experiments was conducted with a pair of spheres oscillating in phase.

A. Flow field around a single oscillating sphere

An example of the streaming flow around an oscillating sphere in the center of the tank is shown in Fig. 3. Images are taken once per oscillation at the center of the stroke, and then three dimensional positions of the tracer particles are determined. The cylindrical symmetry of the problem allows us to present the entire flow field by combining particles at all azimuthal angles, φ , and plotting their height, z , vs. the distance from the oscillation axis, r . Plots of v_φ and horizontal cuts confirm that the motion is almost entirely in the $r - z$ plane in our experiments. (There are weak variations in the azimuthal direction, a result of convection currents, which lead to crossing tracks in regions of slow streaming flow in the z - r -plots.) The radial velocity component v_r is shown in color. A few streamlines have been drawn in to indicate the direction of flow. The particle tracking was optimized to observe the outer recirculations which cause the attractive interactions between particles. These flows are much weaker than the inner recirculations, so this data does not resolve the inner recirculation zones. There are some mismatched particles resulting in a background of short spurious tracks, for example those inside the sphere.

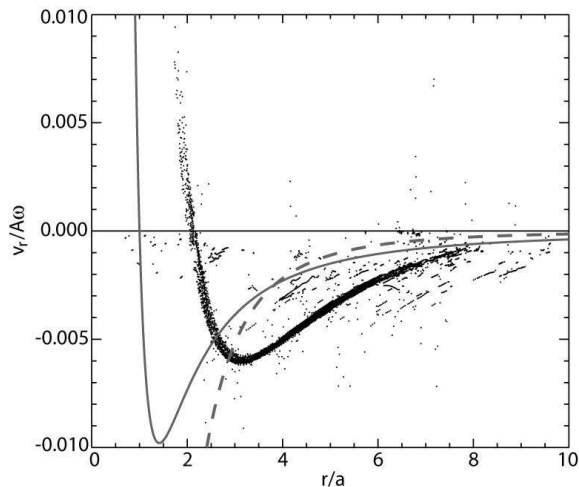


FIG. 4: Steady inflow velocity v_r vs. r in a small stripe around $z = 0$. The scattered points are experimental data ($Re = 30$, $\epsilon = 1.4$, $R_s = 42$, $|M|^2 = 21.4$), and are compared to the theoretical calculations of Brenner/Stone (dashed line) and Riley (solid line; NOTE: divided by 50 to fit on the plot). Background points are bad stereoscopic matches and should be ignored.

1. Streaming velocity in the equatorial plane

Figure 4 shows the measured radial streaming velocity as a function of radius for particles within 0.5cm of the equatorial plane. The flow is attractive at large distances with a stagnation point 2cm from the center of the sphere. This figure also shows two theoretical calculations of the streaming velocity. Riley¹⁰ predicts that flows in limit II (from Fig. 1) have

$$\frac{u_r(r, z = 0)}{A\omega} = -\frac{45}{32} \frac{\epsilon a^2}{r^2} \left(1 - \frac{a^2}{r^2}\right), \quad (4)$$

whereas Brenner and Stone⁶ predict that flows in limit III have

$$\frac{u_r(r, z = 0)}{A\omega} = -0.53 \sqrt{\nu/\omega} \frac{a^2}{r^3}. \quad (5)$$

The agreement of the rate of attraction of two spheres with Eq. 5 was a result from Voth et. al⁶.

Figure 4 reveals a strong discrepancy between the theories and our experiment. The Brenner and Stone results (dashed line) has the right order of magnitude, but a significantly different functional form. Riley's result (solid line) has been divided by 50 to make it fit on the graph. The reason for the discrepancy is partly the impossibility of realizing an infinitesimal amplitude in the experiment. We think that the Brenner and Stone result does better because the experiment at $Re_s = 42$ is closer to the high Re_s limit than it is to the infinitesimal Re_s limit used by Riley. However, viscous effects are likely still important in this Re_s range. Clearly, the inflow velocity in

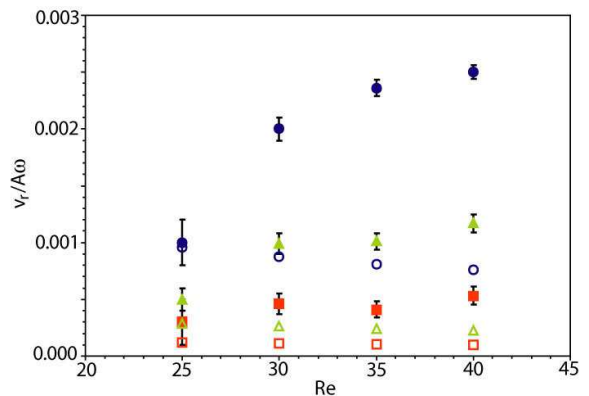


FIG. 5: Steady inflow velocity v_r as a function of Re at fixed $\epsilon = 0.7$. A comparison between the experiment (filled shapes) and the Brenner/Stone-theory (open shapes) measured at $4a$ (circles), $6a$ (triangles), and $8a$ (squares) from the center of the sphere.

the range $r = a - 5a$ is not adequately captured by the available theories, and this is the range relevant for the experiments in Voth et. al⁶. Blackburn⁹ has simulated the flow around oscillating spheres and presents similar profiles of cycle-average radial velocities. His results also disagree with both of the theoretical predictions, but appear to be consistent with our experiments. However, a direct comparison is not possible as his choices of oscillation amplitude, $\epsilon = 0.1$ and 10 , are inaccessible to the experiment.

The dependence of the equatorial velocity on Re is shown in Figure 5. We plot v_r at $4a$ (four sphere radii away from the center of the sphere), $6a$, and $8a$, and use $\epsilon = 0.7$ (half that of Fig. 4). At each distance, the inflow velocity increases with increasing Re . This is in disagreement with Eq. 5 which predicts the velocity should decrease with increasing Re as $u_r/(A\omega) = -0.53(Re/2\epsilon)^{-1/2}(a/r)^3$. This discrepancy may be a result of viscous effects on the streaming flow which are ignored in the potential flow solution used to obtain Eq. 5. Another feature of the inflow velocity is that it does increase with increasing oscillation amplitude ϵ at fixed Re ¹⁶, but does not closely match either the linear dependence of Eq. 4 or the square root dependence above.

2. Position of the equatorial stagnation point

The stagnation point, where the inner and outer recirculation zones meet in the equatorial plane, can be seen in Figures 3 and 4. The position of the stagnation point, r_s , as a function of the Reynolds number Re is shown in Figure 6. Several runs are shown with different amplitudes and different sphere diameters. As Re is increasing, the stagnation point moves closer to the sphere, which is expected since the oscillatory boundary layer thickness is decreasing: $\delta_{osc} = \sqrt{\nu/\omega} = a(2\epsilon)^{1/2}Re^{-1/2}$.

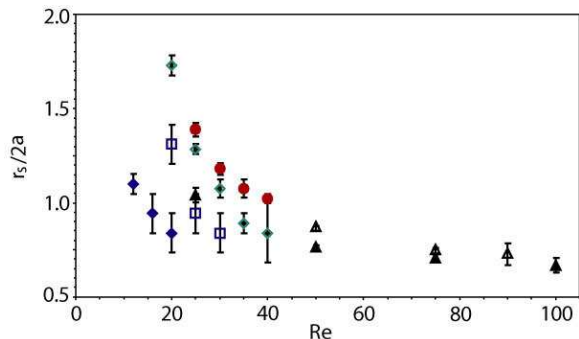


FIG. 6: Position of the stagnation point r_s as a function of Re at different A/a . Filled diamond: $A/a = 0.16$, $2a = 2\text{cm}$; filled triangle: $A/a = 0.3$, $2a = 5\text{cm}$; open triangle: $A/a = 0.5$, $2a = 5\text{cm}$; filled circle: $A/a = 0.7$, $2a = 2\text{cm}$; open diamond: $A/a = 1.4$, $2a = 2\text{cm}$; open square: $A/a = 2$, $2a = 2\text{cm}$. Note that r_s is measured from the center of the sphere, so the surface of the sphere is at 0.5 on the graph.

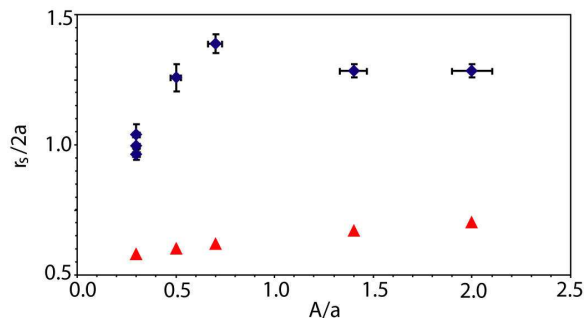


FIG. 7: Position of the stagnation point r_s as a function of A/a at fixed $Re = 25$. The triangles are one oscillatory boundary layer thickness, δ_{osc} , beyond the surface of the sphere. The surface of the sphere is located at 0.5.

The position of the stagnation point already reveals a problem with previous interpretations of the attractive interactions between spheres. In Voth et. al⁶ the spheres attract to contact at approximately $Re < 7$ and $\epsilon < 1.4$. Our data, at $Re = 20$ and $\epsilon = 1.4$, shows that the stagnation point is 1.7 diameters from the center of the sphere. At lower Re , the stagnation point should extend farther. We conclude that the repulsive flow inside the stagnation point extends across the distances where attraction was observed in Ref.⁶. Therefore, something more than simple advection by the single particle streaming flow must be involved in the fluid mediated attraction.

The dependence of the position of the stagnation point on oscillation amplitude is shown in Fig. 7. The size of the two inner recirculation zones has a maximum just below $A/a = 1$, which is in contrast to the monotonic increase in the oscillatory boundary thickness. The reasons for this non-monotonic behavior are not fully understood. As the steady streaming velocity increases with increasing ϵ , the steady boundary layer may become thin-

ner which counteracts the increasing thickness of the oscillatory boundary layer. An analytic solution for the streaming flow with non-infinitesimal oscillation amplitude would be very helpful in further understanding of these issues.

B. Changes of the flow field due to the bottom plate

The next set of experiments brought the sphere closer to the bottom plate of the tank. We took 5 single sequences each having a different distance, d , from the bottom plate (see Fig. 2) with fixed Reynolds number and amplitude ($Re = 30$, $\epsilon = 0.7$). Figure 8 shows that not only was the flow geometry distorted by the presence of the boundary, but the topology also completely changed. The lower of the two far field recirculation zones successively closes in, gets compressed and eventually joins the upper of the two inner recirculation zones. Earlier we have used the position of the stagnation point to separate the inner repulsive recirculation and the outer attractive flow. Here, this stagnation point has disappeared. An animation of the phase dependence of the flow topology for Fig. 8(d) is available online¹⁷.

C. Implications for interpreting fluid mediated interactions between oscillating particles

The streaming flow in Fig. 8 gives a vantage point from which we can evaluate the role of streaming flows in the fluid mediated particle interactions reported in References^{6,7}. Because of the topology change that unites one of the outer recirculations with an inner recirculation, the repulsive part of the the flow extends much farther from the sphere than it does when the wall is not present. Even without the wall, the repulsive flow extended too far from the sphere to explain the attraction observed in Voth et. al⁶. Now near the bottom wall, the repulsive region extends to $r = 4a$ and covers most of the attractive range. The current data is at higher Reynolds number ($Re = 30$ compared with $Re 10$), but Fig. 6 shows that the extent of the repulsive recirculation extends even farther at lower Re . The failure of Eq. 5 to describe the attractive flow velocity further indicates that the attraction and repulsion between vertically vibrated particles cannot be explained purely by advecting the particles in the single particle flow fields. We conclude that the interactions previously observed^{6,7} are the result of nonlinear interactions between the flows around multiple particles. This conclusion has also been drawn from the study of the horizontally vibrated system by Klotsa et. al¹⁸.

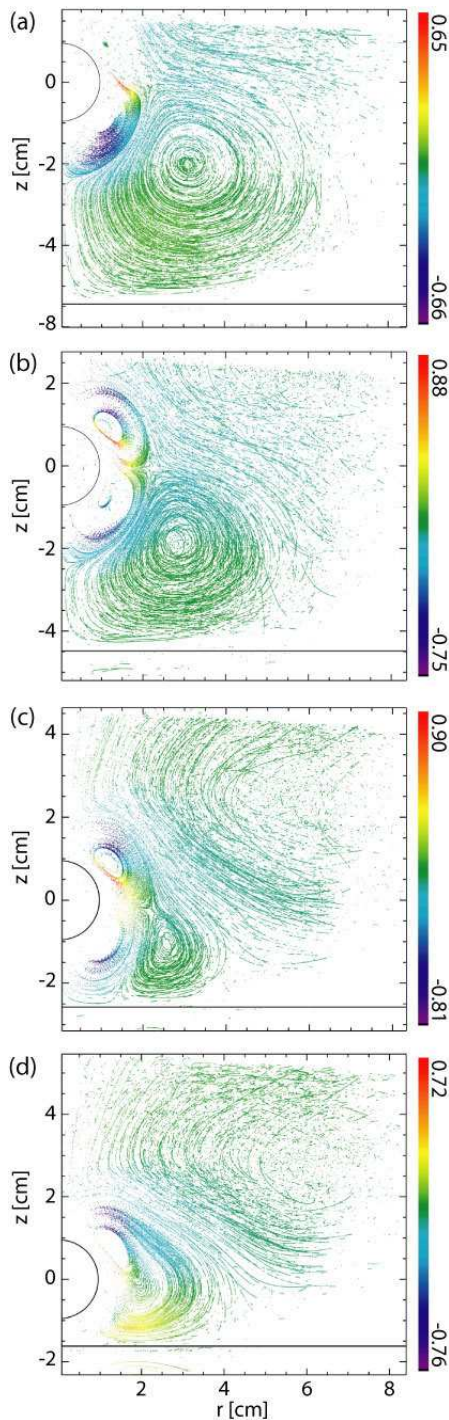


FIG. 8: Changes to the streaming flow geometry as the sphere oscillates closer to the bottom wall of the container with fixed $\epsilon = 0.7$ and $Re = 30$. The plot shows height vs. radial position and the color indicates the radial velocity component, v_r . For (a) $d/2a = 2.0$, (b) = 1.5, (c) = 0.5, and (d) = 0.0. For each image the center of the sphere is at $z = 0$, and the sphere is at the center of the rod stroke. In (d) the sphere is almost touching the bottom wall at the bottom of its stroke. The position of the bottom wall is indicated by the black line.

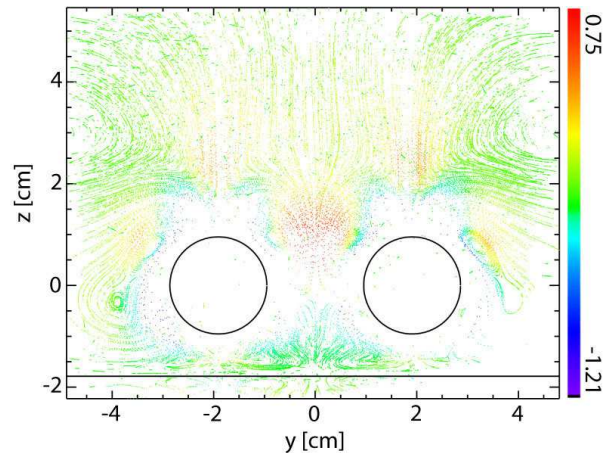


FIG. 9: A periodic displacement plot in a 1-cm thick layer with $Re = 30$ and $A/a = 0.7$. This $x = 0$ -layer is $-0.5 < x < 0.5$. The plot shows y vs z and the color indicates the height velocity component, v_z . The position and size of the spheres are indicated by the semicircles.

D. Flow field around 2 spheres

Since non-linear interactions between the flows around two spheres must be responsible for the attractive and repulsive interactions, we have measured the flow around two oscillating spheres. The flow is now fully three dimensional, which makes full use of the capabilities of 3DPTV. We mounted two spheres on separate vertical rods and vibrated them in phase with a fixed distance of roughly 1 sphere diameter, $2a = 1.91\text{cm}$, between them. Figure 9 shows the flow around two oscillating spheres near the bottom of the tank. Since this flow is not azimuthally symmetric we plot only a slice of the velocity field that contains the vertical plane going through the centers of both spheres. Producing this image required 10 times more data than the single particle flow fields since it could not be azimuthally averaged. The flow geometry on the left and right edges of Fig. 9 shows roughly the same topology as the case of one sphere near the bottom wall (see Fig. 8). Observation of the full flow field reveals that particles in the equatorial recirculation zone experience azimuthal drift toward the center where they are ejected in the upward jet. A 3D visualization of some of these trajectories is available online¹⁷.

V. CONCLUSIONS

We have demonstrated that a simple implementation of three dimensional particle tracking can provide accurate measurements of the flow fields around oscillating spheres. We set out to deepen our understanding of the fluid mediated attraction and repulsion between particles oscillating in a fluid, building on work by Voth et al⁶. This earlier work had observed clustering of particles os-

cillated in a fluid, and found that for some parameters there could be repulsion and intriguing dynamic states. It also proposed that the attraction could be described by an analytical calculation of the streaming flow around single spheres.

For parameters typical of the experimental observations of fluid mediated interactions, our measured velocity fields are quite different from available analytical calculations. This discrepancy is probably due to the theories being derived for limiting cases that do not adequately match experimental parameters. When a sphere is oscillating perpendicular to a flat plate, the streaming flow undergoes a dramatic change in topology due to the coalescence of two recirculation zones. This expands the range of the repulsive streaming flow near the sphere. Together these conclusions demonstrate that previous explanations⁶ gave oversimplified descriptions of the flows that lead to the interactions between spheres. Some parts

of the interactions can be qualitatively understood by single particle streaming flows. However, two particle effects are important in controlling the interactions of particles within a few diameters of each other at the studied parameters. We have presented measurements of the streaming flow around a pair of oscillating spheres, but more work remains to be done in understanding how the non-linear interaction of the oscillatory flows leads to observed interactions between oscillating spheres.

VI. ACKNOWLEDGEMENTS

This work was supported by Wesleyan University and NSF Grant DMR-0547712. We appreciate discussions with Michael Brenner and Jerry Gollub.

* Currently at Institut für Experimentelle und Angewandte Physik, Universität Regensburg, D-93040 Regensburg, Germany

† URL: <http://gvoth.web.wesleyan.edu/lab.htm>

¹ Lord Rayleigh. On the circulation of air observed in Kundt's tubes and some allied acoustical problems. *Philos. Trans. R. Soc. London Ser. A*, 175.

² H. C. Starritt, F. A. Duck, and V. F. Humphrey. An experimental investigation of streaming in pulsed diagnostic ultrasound beams. *Ultrasound in Medicine and Biology*, 15(4):363–373, 1989.

³ P. Marmottant and S. Hilgenfeldt. A bubble-driven microfluidic transport element for bioengineering. *Proceedings of the National Academy of Sciences*, 101(26):9523–9527, 2004.

⁴ P. Marmottant and S. Hilgenfeldt. Controlled vesicle deformation and lysis by single oscillating bubbles. *Nature*, 423:153–156, 2003.

⁵ J. Lighthill. Acoustic streaming in the ear itself. *Journal of Fluid Mechanics*, 239:551–606, 1992.

⁶ G. A. Voth, B. Bigger, M. R. Buckley, W. Losert, M. P. Brenner, H. A. Stone, and J. P. Gollub. Ordered clusters and dynamical states of particles in a vibrated fluid. *Physical Review Letters*, 88:234–301, 2002.

⁷ C. C. Thomas and J. P. Gollub. Structures and chaotic fluctuations of granular clusters in a vibrated fluid layer. *Physical Review E*, 70(6):1305, 2004.

⁸ R. Wunenburger, V. Carrier, and Y. Garrabos. Periodic order induced by horizontal vibrations in a two-dimensional assembly of heavy beads in water. *Physics of Fluids*, 14(7):2350–2359, 2002.

⁹ H. M. Blackburn. Mass and momentum transport from a

sphere in steady and oscillatory flows. *Physics of Fluids*, 14(11), 2002.

¹⁰ N. Riley. On a sphere oscillating in a viscous fluid. *Quarterly Journal of Mechanics and Applied Mathematics*, XIX(4), 1966.

¹¹ M. Van Dyke. *An album of fluid motion*. The Parabolic Press, 1982.

¹² T. Dracos, editor. *Three-Dimensional Velocity and Vorticity Measuring and Image Analysis Techniques*. Kluwer Academic Publishers, Netherlands, 1996.

¹³ S. Ott and J. Mann. An experimental investigation of the relative diffusion of particle pairs in three-dimensional turbulent flow. *Journal of Fluid Mechanics*, 422:207–223, 2000.

¹⁴ B. Luthi, A. Tsinober, and W. Kinzelbach. Lagrangian measurement of vorticity dynamics in turbulent flow. *Journal of Fluid Mechanics*, 528:87–118, 2005.

¹⁵ M. Bourgoïn, N. T. Ouellette, H. Xu, J. Berg, and E. Bodenschatz. The role of pair dispersion in turbulent flow. *Science*, 311:838–840.

¹⁶ F. Otto. Exploration of the flow field around an oscillating sphere using 3d particle tracking velocimetry. Master's thesis, Universität Regensburg, 2004.

¹⁷ Video animations showing the phase movement of Fig. 8(d), and the 3D trajectories of particles around two spheres (as discussed in Sec. IV B) can be found at (<http://gvoth.web.wesleyan.edu/oscillatingsphere>).

¹⁸ D. Klotsa, Michael R. Swift, R. M. Bowley, and P. J. King. The interaction of spheres in oscillatory fluid flows. *PREPRINT*, 2007.